

Self-magnetic compensation and shifted hysteresis loops in ferromagnetic samarium systems

P. D. Kulkarni,¹ S. K. Dhar,¹ A. Provino,² P. Manfrinetti,² and A. K. Grover¹

¹*Department of Condensed Matter Physics and Materials Science, Tata Institute of Fundamental Research, Homi Bhabha Road, Colaba, Mumbai 400005, India*

²*CNR-SPIN and Dipartimento di Chimica e Chimica Industriale, Università degli Studi di Genova, Via Dodecaneso 31, Genova 16146, Italy*

(Received 1 July 2010; revised manuscript received 19 August 2010; published 5 October 2010)

For Sm^{3+} ions in a vast majority of metallic systems, the following interesting scenario has been conjured up for long, namely, a magnetic lattice of tiny self- (spin-orbital) compensated $4f$ -moments exchange coupled (and phase reversed) to the polarization in the conduction band. We report here the identification of a self-compensation behavior in a variety of ferromagnetic Sm intermetallics via the fingerprint of a shift in the magnetic hysteresis (M - H) loop from the origin. Such an attribute, designated as exchange bias in the context of ferromagnetic/antiferromagnetic multilayers, accords these compounds a potential for niche applications in spintronics. We also present results on magnetic compensation behavior on small Gd doping (2.5 at. %) in one of the Sm ferromagnets (viz., SmCu_4Pd). The doped system responds like a pseudoferrimagnet and it displays a characteristic left-shifted linear M - H plot for an antiferromagnet.

DOI: [10.1103/PhysRevB.82.144411](https://doi.org/10.1103/PhysRevB.82.144411)

PACS number(s): 75.50.Cc, 75.60.-d, 71.20.Lp

I. INTRODUCTION

Samarium is the fifth member of the $4f$ -rare earth (R) series, in which spin-orbit (S - L) coupling prevails and the total angular momentum (J) governs the magnetic moment. In particular, for free Sm^{3+} ion ($S=5/2$, $L=5$, $J=5/2$, and Lande's g -factor, $g_J=2/7$), the $4f$ -orbital contribution [$-\mu_B\langle L_z \rangle = -\mu_B J(g_J - 2)$] to the magnetic moment is only 20% larger than its $4f$ -spin [$|\mu_B 2\langle S_z \rangle| = 2\mu_B J(1 - g_J)$] contribution, this renders it a small magnetic moment ($\mu_J = g_J J$) of $5/7\mu_B$.¹ In a crystalline environment, the degeneracy of the ground J multiplet is partially lifted, and in the specific case of the Sm^{3+} ions, the crystalline electric field and the exchange field can induce admixture of the higher J -multiplets ($J=7/2, 9/2$) into the ground J multiplet ($J=5/2$).²⁻⁵ Such circumstances not only substantially reduce the magnetic moment/ Sm^{3+} ion⁶⁻⁹ but also make the orbital and spin contributions undergo different thermal evolutions.^{4,5,8,10,11}

Enigmatic magnetic characteristics of Sm^{3+} ion were first recognized by White and Van Vleck in early 1960s,² as they explored a ramification of the relatively small separation between the ground J multiplet ($J=5/2$) and the first excited state ($J=7/2$). On allowing for the admixture of higher J multiplet into the ground J multiplet by the perturbation of an exchange field, they could demonstrate² the breakdown of the proportionality between the thermal evolution of bulk magnetic susceptibility ($\langle \mu_z \rangle = -\mu_R \langle J_z \rangle$) and the local $4f$ -spin susceptibility ($\propto \langle S_z \rangle$) as measured by the NMR Knight shifts. White and Van Vleck's work was extended further in 1970s (see, e.g., our Refs. 4-7 by adding the role of crystalline electric fields to the admixture effects, and it was calculated^{6,7} that the saturation magnetic moment at Sm^{3+} ion could indeed vanish, with opposing orbital and spin contributions canceling out each other, under some parametric conditions involving the crystalline electric fields and the exchange field. There were no very clear experimental elucidations of the said near cancellation.

Our rationale for the assertion of the self-compensation behavior in Sm systems via the identification of shift in the

M - H loop from origin now stems from a recent exploration by some of us¹² in a single crystal of admixed rare-earth intermetallic, viz., $\text{Nd}_{0.75}\text{Ho}_{0.25}\text{Al}_2$, derived from a ferromagnetic RAl_2 series of compounds. It is well documented that the $4f$ spins of the dissimilar R^{3+} ions in such admixed rare-earth intermetallics continue to remain ferromagnetically coupled,¹³⁻¹⁵ which, in turn, mandates an antiferromagnetic coupling between the magnetic moments of dissimilar R^{3+} ions belonging to the first half and the second half of the $4f$ series, for which $J=L-S$ and $J=L+S$, respectively, in the ground state. The Nd^{3+} and Ho^{3+} ions in the case cited above belong to the first/second half of $4f$ series. The admixed $\text{Nd}_{0.75}\text{Ho}_{0.25}\text{Al}_2$ alloy, where $\mu_{\text{Nd}} \approx 2.5\mu_B$ and $\mu_{\text{Ho}} \approx 8.5\mu_B$, therefore responds like a ferrimagnet¹⁶ and displays a "magnetic compensation characteristic." In close proximity of the compensation temperature (T_{comp}), the opposing contributions to the magnetization signal from the two pseudosublattices of Nd^{3+} and Ho^{3+} ions nearly balance out, as in a (quasi)antiferromagnet.¹² A very striking observation, however, is the surfacing up¹² of the left/right shift [i.e., finite exchange-bias (EB) -like effect] usually seen in ferro/antiferromagnetic multilayers¹⁷ over a small temperature interval encompassing the T_{comp} in $\text{Nd}_{0.75}\text{Ho}_{0.25}\text{Al}_2$. The presence of such an EB-like effect in very close proximity of its T_{comp} , and, importantly, its sign change across it, correlates with the reversal in the orientation of the conduction electron polarization with respect to the externally applied field.¹² On drawing an analogy between the EB-like effect observed over a narrow interval in $\text{Nd}_{0.75}\text{Ho}_{0.25}\text{Al}_2$ with the relevant observation to be reported ahead in several Sm ferromagnets, the notion of a near self-compensation for the local moment of Sm^{3+} in them would straight away become evident. We will first present the experimental results in a variety of Sm ferromagnets to validate the nomenclature of "near self-magnetic compensation." Thereafter, we shall also elucidate the phenomenon of phase reversal in the EB in one of the chosen Sm systems, when it is substitutionally doped with few percent of Gd^{3+} ions. The doped system imbibes magnetic compensation phenomenon as in pseudoferrimagnets,

which is in addition to the near self-compensation happening at Sm^{3+} ion. The quasilinear M - H data in the doped system displays left shift as well as right shift from the origin as a function of temperature.

II. EXPERIMENTAL

A. Sample preparation and characterization

Polycrystalline samples of SmCu_4Pd , SmPtZn , SmCd , SmZn , SmScGe , and SmAl_2 were prepared by melting together stoichiometric amounts of the constituent elements in a sealed tantalum crucible in an induction furnace, following usual special care and procedure for handling volatile samarium metal.^{18,19} Samarium, scandium, and gadolinium metals were of 99.9 wt % purity. Aluminium, copper, zinc, cadmium, and germanium were of 99.999 wt % purity and palladium and platinum of purity 99.9 wt % were in powder form ($<60 \mu\text{m}$ powder) to start with. While weighing, small pieces of distilled Sm and turnings of scandium and gadolinium were handled under pure argon to minimize the possibility of exposure to air. The melting in the induction furnace was slowly progressed, the melt was shaken to ensure homogenization of the constituents. The melting stage was repeated at least twice. To avoid the reaction of the melt to the crucible in the case of SmScGe , the binary alloy ScGe was initially prepared by arc melting and to it an appropriate amount of Sm was added, before sealing the reactants in a tantalum crucible. Different specimen were given different heating and annealing treatments, following earlier leads in the literature.^{10,18,19} the binary SmZn and SmCd were induction heated up to 1100 °C, followed by annealing in evacuated sealed quartz tube at 920 °C for 3 days. SmScGe was heated up to 1700 °C, followed by vacuum annealing at 900 °C for 4 days. The newly synthesized SmPtZn for the present study was induction heated up to 1400–1500 °C, followed by annealing at 800 °C for 7 days. The samples of the admixed $\text{Sm}_{1-x}\text{Gd}_x\text{Cu}_4\text{Pd}$ ($x=0.01, 0.015, 0.02, 0.025, 0.03, \text{ and } 0.04$) were prepared by melting together appropriate amounts of the end members, SmCu_4Pd and GdCu_4Pd . All the polycrystalline samples were checked by both metallographic examination of the small pieces of the ingots and by recording x-ray diffraction patterns of all the specimen finely crushed in an inert atmosphere. As a result of the preparation method and the annealing sequence adopted, each sample was confirmed to have been formed in the desired crystallographic phase. No evidence of strong sample texturing was noted in any of the samples. In few alloy buttons, very low amount (1–3 %) of extra phase(s) could, however, be seen as narrow grain separation.

The intermetallics, SmCd and SmZn , crystallize in cubic (B2) CsCl structure,⁸ SmAl_2 and SmCu_4Pd have cubic MgCu_2 (Ref. 13) (C15 Laves phase) and cubic MgCu_4Sn structures,¹⁸ respectively. SmScGe and SmPtZn have tetragonal CeScSi-type¹⁹ and orthorhombic TiNiSi-type²⁰ structures, respectively. The intermetallic SmPtZn has been newly synthesized for the present study, its lattice parameters are $a=7.015(2) \text{ \AA}$, $b=4.220(1) \text{ \AA}$, and $c=8.111(3) \text{ \AA}$. In SmCd and SmZn , the Sm^{3+} ions form a simple cubic lattice, in SmCu_4Pd and SmAl_2 , they form face-centered-cubic (fcc)

and diamond structures, respectively. In SmScGe and SmPtZn , Sm^{3+} ions yield tetragonal and orthorhombic sublattices, respectively.

B. Magnetization measurements

For the magnetization measurements, a sample piece (20–100 mg) was cut from a given ingot and loaded in the straw holder. Magnetization measurements were performed using a superconducting quantum interference device (SQUID)-vibrating sample magnetometer (Model S-VSM) of Quantum Design, Inc., U.S.A. In S-VSM, a sample vibrates along the axis of the cylindrical second derivative coil array. The SQUID sensor in S-VSM can detect a signal as low as 10^{-7} emu and the magnetization signal from the blank straw holder is $\sim 2 \times 10^{-7}$ emu. In the paramagnetic state, the signal from a sample of ~ 20 mg is on the order of 10^{-5} emu at $H \sim 10$ Oe, and this signal enhances by 2–3 orders of magnitude in the magnetically ordered state below T_c . The remanent field(s) trapped inside the superconducting magnet was ascertained by recording the M - H data while ramping the field down across the zero position from both positive and negative sides for the standard paramagnetic Pd sample. These corrections were incorporated while plotting the M - H data for the experimental samples. We anticipate that the error in the location of the zero-field position during different cycles in a given specimen is limited to within 1–2 Oe. The determined values of the effective coercive field and the exchange-bias field are reliable to within 2 Oe.

III. RESULTS AND DISCUSSION

A. Magnetization measurements in pristine ferromagnetic samarium intermetallics and the fingerprint of exchange bias

Figure 1 shows the M - H loops in polycrystalline samples of six Sm-based ferromagnets at the temperatures as indicated. All the M - H loops in Figs. 1(a)–1(f) were obtained by ramping the field between $\pm H_{max}$, after initially cooling a given sample to a selected temperature in a field of chosen H_{max} . The panels (a)–(f) in Fig. 2 display the temperature variations of the magnetization (M vs T) measured in a field of 10 kOe in the six samples. The ferromagnetic T_c values ascertained from the very low field ($H \sim 10$ Oe) M - T curves (not shown here) in the respective samples have been indicated in the plots displayed in Fig. 2.

The M - H loops at $T \ll T_c$ in the Figs. 1(a)–1(e) are clearly asymmetric, their centres of gravity are left shifted as the field value of crossover of the $M=0$ axis while ramping the field down (i.e., H_-) is larger in magnitude than the corresponding value while ramping the field up (i.e., H_+). We identify the EB field as $H_{EB} = -(H_- + H_+)/2$ (Ref. 17) so that it is deemed as positive/negative for the left/right shifted M - H loop. The M - H loop in Fig. 1(f) for SmAl_2 ($T_c = 125$ K) at 20 K appears symmetric, however, it also yields $H_{EB} = +50$ Oe, a left-shifted value, much lower than the H_{EB} values indicated in the Figs. 1(a)–1(e) in the other Sm ferromagnets. H_{EB} value at a given temperature in a given compound depends somewhat on the value of initial cooling field and the chosen H_{max} . Typically, up to 10% change in a given

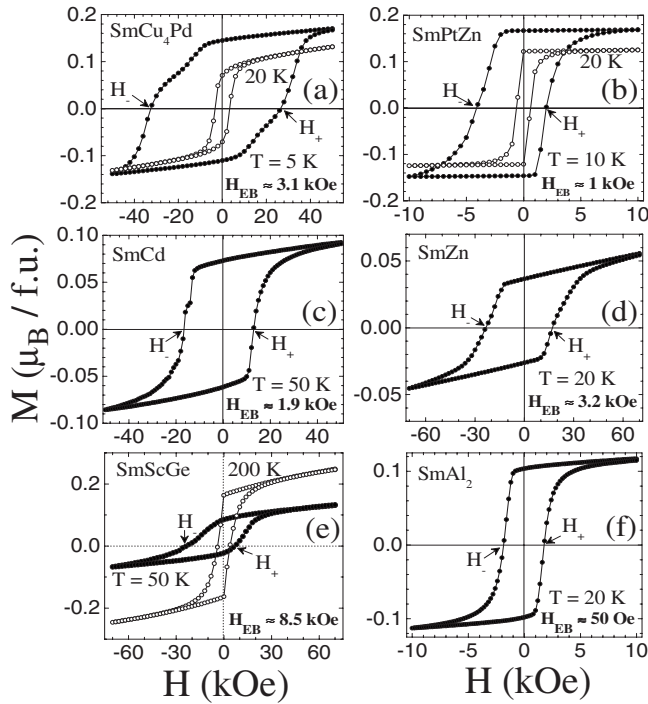


FIG. 1. M - H loops at selected temperatures ($<T_c$) in (a) SmCu_4Pd , (b) SmPtZn , (c) SmCd , (d) SmZn , (e) SmScGe , and (f) SmAl_2 . The exchange-bias field [$H_{\text{EB}} = -(H_- + H_+)/2$], which measures the left shift in a given M - H loop at a given temperature, is stated in each of the panels, (a)–(f).

H_{EB} value could be noted on changing the initial field in which a sample is cooled and thereafter varying the H_{max} up to 70 kOe, the highest field available to us in the Quantum Design Inc. S-VSM system.

It is fruitful to examine the small magnetic moment values in Figs. 1(a)–1(f), in addition to the presence of EB-like effect in them. Adachi *et al.*⁸ had determined conduction-electron polarization (CEP) in SmCd , SmZn , and SmAl_2 to be antiferromagnetically linked to the net local moment of the Sm^{3+} ions. The CEP contributions at $T=0$ K range between 0.2 and $0.4\mu_B$ whereas Sm magnetic moment values are calculated⁸ to lie between 0.3 and $0.5\mu_B$. In ferromagnetic GdCu_4Pd and GdScGe , the magnetic moment per formula unit values are above $7.6\mu_B$,^{18,21} thereby, elucidating that the contribution from polarized conduction electron adds on to the local moment of $7\mu_B/\text{Gd}^{3+}$ in them. This, in turn, implies that the CEP contribution in SmScGe and SmCu_4Pd would also be in phase⁹ with the contribution from the $4f$ spin of Sm^{3+} and out of phase with net $4f$ -magnetic moment of Sm^{3+} ion. Continuing in the same vein, note further the nearly saturated value of $0.2\mu_B/\text{f.u.}$ in newly synthesized SmPtZn in Fig. 1(b); its smallness once again attests to the competition between the contributions to the magnetization signal from the local $4f$ -magnetic moment of Sm^{3+} and that from the CEP.

Another instructive observation is the contrast in the shape of M - T curves in Figs. 2(a), 2(b), and 2(f) with that of the M - T curves in Figs. 2(c)–2(e). The former shape reflects the monotonic increase in the magnetization expected in ferromagnets whereas the latter nonmonotonic peaklike re-

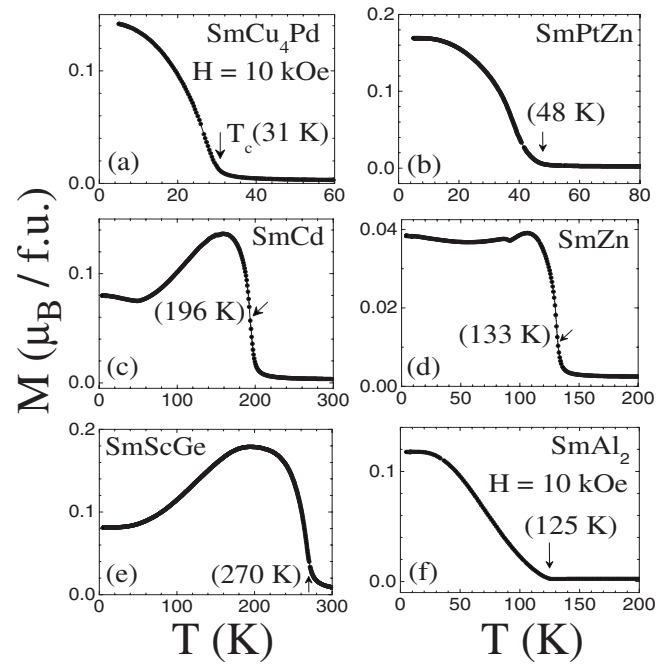


FIG. 2. M vs T measured while cooling down in a field of 10 kOe in different Sm compounds. T_c values determined from the low field ($H \sim 10$ Oe) M - T curves (not shown here) are indicated with arrows.

sponse is akin to that usually seen in ferrimagnets. We recall here that Adachi *et al.*⁸ pointed out that while SmAl_2 [cf. Fig. 1(f)] is a usual “orbital-surplus” Sm ferromagnet; in SmCd [cf. Fig. 1(c)] as well as in SmZn [cf. Fig. 1(d)], the contribution to the total magnetization from the local magnetic moment of Sm^{3+} at $T=0$ K was calculated to be only ($\sim 0.35\mu_B$), which is smaller than the calculated contribution ($\sim 0.4\mu_B$) from the CEP. The local moment contribution is phase reversed to the CEP contribution in Sm ferromagnets under study. The latter two compounds, viz., SmCd and SmZn , were thereby termed as “spin-surplus” Sm ferromagnets.⁸ In a spin-surplus Sm ferromagnet, the sum of the contributions from the local $4f$ -spin moment and the CEP exceeds that from the local $4f$ -orbital contribution. The opposing “spin” and “orbital” contributions thermally evolve to their respective saturated values at $T=0$ in a monotonic manner on cooling below the T_c , however, the former does so faster than the latter. Such a difference in the temperature dependences of the spin and the orbital contributions can yield a peaklike characteristic in the M - T curve of a spin-surplus Sm ferromagnet.^{8,10} It is worth reiterating that CEP contribution is aligned along the applied field in the spin-surplus situation and phase reversed to it in the orbital-surplus ferromagnets. Extending the reasoning further, the differences in the contours of the M - T curves in Figs. 2(a), 2(b), and 2(f) in the orbital-surplus cases also reflect the differences in the thermal evolution of contributions from the $4f$ -orbital and the $4f$ -spin parts to the magnetization of the Sm^{3+} ion in different crystallographic environment and under the influence of different exchange field values.

Figures 3(a) and 3(b) summarize the temperature variations of exchange-bias field [$H_{\text{EB}}(T)$] in the orbital-surplus

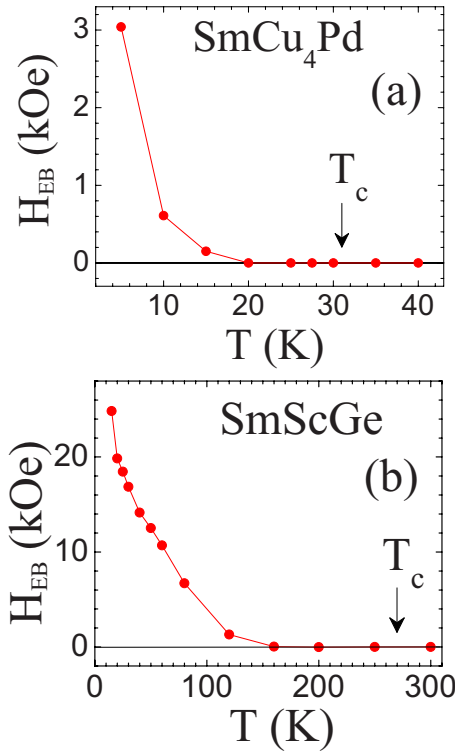


FIG. 3. (Color online) Temperature variation of left shift, i.e., exchange-bias field in ferromagnets (a) SmCu_4Pd and (b) SmScGe . The respective T_c values are indicated with arrows.

SmCu_4Pd ($T_c \approx 31$ K) and spin-surplus SmScGe ($T_c \approx 270$ K) systems. It can be immediately seen that the shift in the hysteresis starts to build up well below the respective T_c values. Our premise that an exchange-bias fingerprints the underlying approach to compensation between the local $4f$ -orbital and $4f$ -spin contribution to the magnetic moment of Sm^{3+} , therefore, implies that it takes a while before the near self-compensation stage gets attained on cooling below T_c . Note further that the shift in hysteresis in both the compounds remain positive down to the lowest temperature. In SmCu_4Pd , H_{EB} values build up to 3 kOe at 5 K whereas, in SmScGe , these values build up to 25 kOe at 15 K.

B. Magnetic compensation phenomenon in a doped samarium ferromagnet and the exchange-bias behavior

It is tempting to conceive a pristine Sm ferromagnet which can display in its thermomagnetic response at low fields the crossover of $M=0$ axis at T_{comp} [see, e.g., the calculated $M-T$ curves in Fig. 1 of Ref. 9] and also exhibit a change in sign of H_{EB} to the negative values across its T_{comp} [similar to the one reported in $\text{Nd}_{0.75}\text{Ho}_{0.25}\text{Al}_2$ (Ref. 12)]. However, magnetic compensation phenomenon has so far not been reported in any pristine Sm ferromagnet. In this context, it is fruitful to explore the occurrence of magnetic compensation behavior and the crossover of left shift in hysteresis to right-shift values in SmCu_4Pd compound by substituting few percent of the Sm^{3+} by the S -state ($L=0$) Gd^{3+} ions. In the doped samarium alloys, the ferromagnetism between the $4f$ spins of Sm^{3+} and Gd^{3+} ions prevails.¹⁵

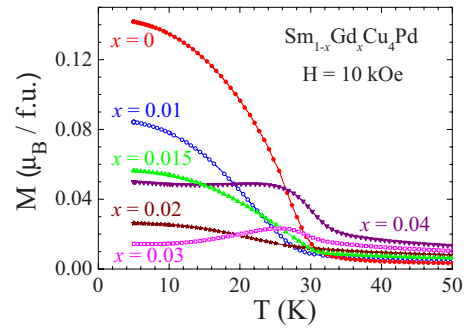


FIG. 4. (Color online) M vs T measured while cooling down in a field of 10 kOe in $\text{Sm}_{1-x}\text{Gd}_x\text{Cu}_4\text{Pd}$ series with $x=0, 0.01, 0.015, 0.02,$ and 0.03 .

The main panel of Fig. 4 shows the $M(T)$ curves at $H = 10$ kOe in spin-ferromagnetic $\text{Sm}_{1-x}\text{Gd}_x\text{Cu}_4\text{Pd}$ alloys for $0 \leq x \leq 0.04$. Note that the magnetization value per formula unit at the lowest temperature decreases from $x=0$ to $x=0.03$. The substitution of Sm^{3+} by Gd^{3+} ions progressively enhances the overall $4f$ -spin contribution vis-à-vis the opposing $4f$ -orbital contribution in the $\text{Sm}_{1-x}\text{Gd}_x\text{Cu}_4\text{Pd}$ matrix. At $x=0.02$, the $M(T)$ response from the T_c end monotonically decreases whereas the $M(T)$ curve for $x=0.03$ has a peaklike shape, akin to that associated with a spin-surplus Sm ferromagnet. These data imply that the magnetic compensation behavior can be observed between $x=0.02$ and $x=0.03$. Figure 5 summarizes the magnetization data in $x=0.025$ sample. Figure 5(a) depicts the $M(T)$ curves in $H = 50$ Oe and 2 kOe, respectively. The crossover of the $M = 0$ axis at $T_{\text{comp}} = 21$ K in the lower field $M(T)$ curve, and the turnaround behavior in the higher field curve at about 21 K in Fig. 5(a) characterize the occurrence of magnetic compensation.

A set of eight panels in Fig. 6 show the portions of the $M-H$ loops between ± 600 Oe in $\text{Sm}_{0.975}\text{Gd}_{0.025}\text{Cu}_4\text{Pd}$ sample at the temperatures identified in Fig. 5 [see the encircled positions, (a)–(h), in this panel]. The sample was initially cooled down in a field of 2 kOe to each temperature, and thereafter the field was ramped between ± 2 kOe. The inset panels in Figs. 6(c) and 6(h) show the representative

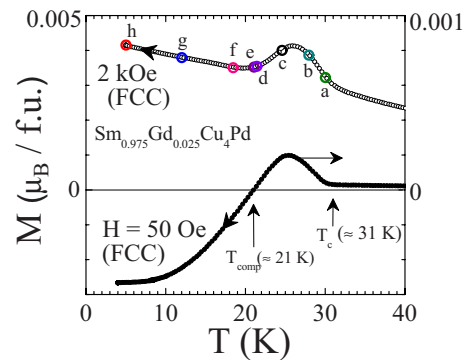


FIG. 5. (Color online) M vs T in $\text{Sm}_{0.975}\text{Gd}_{0.025}\text{Cu}_4\text{Pd}$ at $H = 50$ Oe and 2 kOe. The T_c and T_{comp} values are marked with arrows in low-field fcc curve. The encircled points [from (a)–(h)] on fcc curve at 2 kOe correspond to the temperatures where the $M-H$ loops are traced as shown later in Fig. 6.

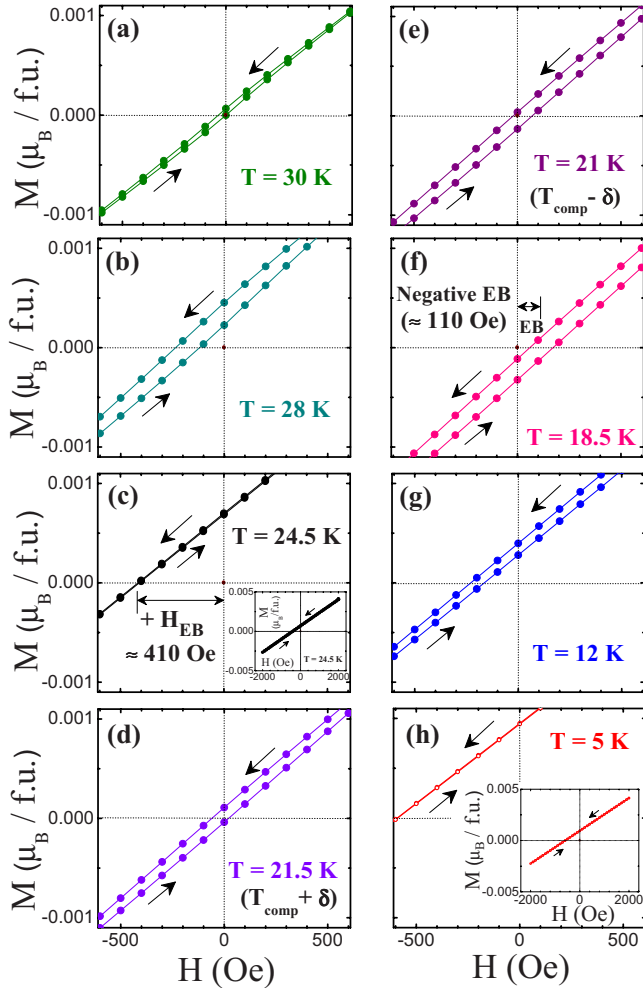


FIG. 6. (Color online) Portions of M vs H loops in $\text{Sm}_{0.975}\text{Gd}_{0.025}\text{Cu}_4\text{Pd}$ at eight different temperatures as indicated in panels (a)–(h). The sample is cooled from above T_c (≈ 31 K) down to the selected temperature and the loop is traced between ± 2 kOe in each case.

M - H data between ± 2 kOe at 24.5 K and 5 K, respectively. Note first the linear nature of the M - H response between ± 2 kOe over the entire temperature range in the magnetically ordered state. This feature, combined with the smallness of the magnetization values, brings out the quasiantiferromagnetic response at this stoichiometry. This is in complete contrast to the ferromagnetic shape of the M - H response (along with the large magnetocrystalline anisotropy and the associated coercivity) in the parent SmCu_4Pd compound [see Fig. 1(a)]. However, the shift in the centre of the gravity (CG) of the M - H data can be noted in different panels of Fig. 6. A tiny left shift in the CG of the M - H data surfaces up at 30 K itself [cf. Fig. 6(a)], which is just below the T_c value of 31 K. The left shift progressively enhances as the temperature lowers further to 24.5 K [cf. Fig. 6(c)]. Interestingly, at 24.5 K, the width of the loop has collapsed. On further lowering the temperature, left shift in CG of the M - H data decreases whereas its width enhances. On lowering temperature below about 21 K ($\approx T_{\text{comp}}$), the left shift crosses over to the right shift [cf. Figs. 6(d) and 6(e)]. The right shift (negative EB) maximizes at 18.5 K [cf. Fig. 6(f)] and, there-

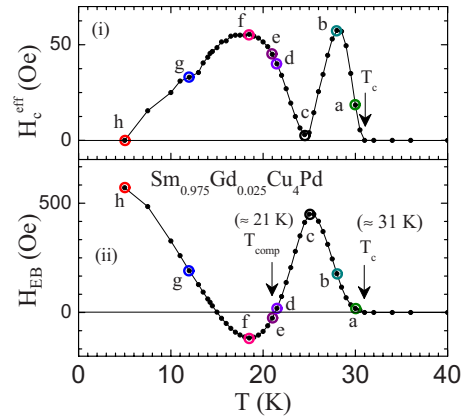


FIG. 7. (Color online) Temperature variation of (a) H_c^{eff} and (b) H_{EB} in $\text{Sm}_{0.975}\text{Gd}_{0.025}\text{Cu}_4\text{Pd}$. The values of H_c^{eff} and H_{EB} are obtained from the M vs H loops of the kind shown in Fig. 6 at various temperatures below T_c (marked with arrow in both panels). The encircled positions in panels (a) and (b) display the selected temperatures at which portions of M vs H loops have been displayed in Fig. 6.

after, it starts to swing backward. On lowering temperature below about 16 K [cf. Fig. 6(g)], the CG of the M - H data returns to the left of the origin [cf. Fig. 6(g) at 12 K]. At 5 K, M - H data once again reaches the collapsed stage [cf. Fig. 6(h)] and H_{EB} value reaches up to ~ 570 Oe.

The two panels [(i) and (ii)] in Fig. 7 summarize the H_c^{eff} [the effective coercive field²² defined as $H_c^{\text{eff}} = -(H_- - H_+)/2$] and H_{EB} values determined from the M - H plots of the kind plotted in Fig. 6. The encircled temperatures in the two panels of Fig. 7 help to identify the respective panels in Fig. 6. It is satisfying to note the occurrence of change in sign of H_{EB} across T_{comp} (≈ 21 K) in panel (ii) of Fig. 7; this characteristic is consistent with the similar behavior across its T_{comp} in the single crystal of $\text{Nd}_{0.75}\text{Ho}_{0.25}\text{Al}_2$. In the latter system, measurable $H_{\text{EB}}(T)$ values exist only in the neighborhood of T_{comp} , where the contributions from the local moments of Nd and Ho ions nearly compensate each other. The observation that appreciable $H_{\text{EB}}(T)$ values exist over the entire temperature range below T_c in $\text{Sm}_{0.975}\text{Gd}_{0.025}\text{Cu}_4\text{Pd}$ implies that compensation between the orbital contribution to the magnetic moment of Sm^{3+} ions and weighted average of spin contributions of local moments of Sm^{3+} and Gd^{3+} ions prevails throughout in the magnetically ordered state. The character of this is quasiantiferromagnetic, as evidenced by the linear M - H data in Fig. 6.

The effective coercive field (H_c^{eff}) in $\text{Sm}_{0.975}\text{Gd}_{0.025}\text{Cu}_4\text{Pd}$ in panel (i) of Fig. 7 registers the collapse in the width of the M - H loop at 24 K, instead of at its T_{comp} value, as noted in the single crystal of $\text{Nd}_{0.75}\text{Ho}_{0.25}\text{Al}_2$ (Ref. 12) and polycrystalline samples of $\text{Pr}_{0.8}\text{Gd}_{0.2}\text{Al}_2$ and $\text{Sm}_{0.98}\text{Gd}_{0.02}\text{Al}_2$.²³ It is useful to recall here that for a soft ferromagnet in contact with a ferrimagnet, Webb *et al.*²² had argued that the effective coercivity diverging from the low- as well as high-temperature ends should collapse on approaching the compensation temperature of the ferrimagnet. The collapse of H_c^{eff} at 24.5 K ($> T_{\text{comp}}$) in the present compound is therefore curious. The location of peak in $H_{\text{EB}}(T)$ at

24.5 K is also a surprise. In any case, the left-shifted linear M - H plots at 24.5 in Fig. 6(c) vividly elucidates the exchange-biaslike notion for an antiferromagnetic system. The Sm moment in the pristine SmCu₄Pd compound is nearly self-compensated below about 20 K (cf. Fig. 3), however, the system retains its orbital-surplus ferromagnetic characteristic over the entire temperature range below T_c . The substitution of 2.5 at. % of Sm³⁺ by Gd³⁺ ions in the doped alloy makes it a pseudoferrimagnet. Between T_c and T_{comp} of 21 K, the doped alloy is *prima facie* spin surplus. The orbital contribution of Sm³⁺ ion overcomes the weighted average of spin contributions of Sm³⁺ and Gd³⁺ ions along with that of the conduction-electron polarization only below T_{comp} of 21 K. The presence of second crossover in $H_{EB}(T)$ in Sm_{0.975}Gd_{0.025}Cu₄Pd near 15 K appears to echo the two crossovers in $H_{EB}(T)$ noted earlier in the compensated polycrystalline samples of Pr_{0.8}Gd_{0.2}Al₂ and Sm_{0.98}Gd_{0.02}Al₂ as well.¹² The complex $H_{EB}(T)$ response in Fig. 7 perhaps arises from an interplay between the approach to self-compensation happening at each Sm³⁺ ion and the competition between the weighted average of residual magnetic moment associated with host Sm³⁺ ions and that of the doped Gd³⁺ ions in the background of polarized conduction band, whose own contribution is an intimate participant in the ongoing competition. We believe that at 24.5 K, $(1-x)|\mu_{Sm}| \approx x|\mu_{Gd}|$ and at T_{comp} of 21 K, in low fields, $(1-x)|\mu_{Sm}| + |\mu_{Gd}| + |\mu_{CEP}| \approx 0$, where $|\mu_{CEP}|$ is the contribution from the conduction-electron polarization. In a larger field (e.g., in 2 kOe), the CEP contribution turns around with respect to the applied field and this could account for the change in sign of H_{EB} across T_{comp} . The rationalization of the second crossover in $H_{EB}(T)$ at 15 K perhaps requires further exploration in a single-crystal sample of the doped Sm system.

IV. SUMMARY AND CONCLUSION

To summarize, we have searched and identified exchange-bias effect in the M - H loops of several ferromagnetic samarium intermetallics having different crystallographic structures. Small (almost) self-compensated local moments of Sm³⁺ ions occupy a unique site in these ferromagnets. The net magnetization values per formula unit in these compounds are small as the conduction-electron polarization competes as well with the contribution from the tiny local moment of Sm³⁺ ions. One of the ferromagnetic Sm compounds is driven to yield a magnetic compensation characteristic by substitutional replacement of few percent of Sm³⁺ by the Gd³⁺ ions. In the compensated stoichiometry, the EB-like field is elucidated to change sign across T_{comp} and echo the recent findings.^{12,23} The behavior in the Sm compounds is generic and has the potential for niche applications of magnetically ordered materials having large spin polarization, negligible self-stray field and the tunable exchange bias. A spin-valve device in spintronics typically incorporates a free ferromagnetic layer and a pinned ferromagnetic layer, exchange coupled to an antiferromagnetic bilayer.²⁴ In such a device, the pinned multilayer portion of the composite could be considered for replacement by a layer of the zero-magnetization Sm ferromagnet.

ACKNOWLEDGMENTS

We acknowledge fruitful discussions with S. Ramakrishnan, S. Venkatesh, A. Thamizhavel, Vikram Tripathi, Gianni Blatter, T. Nakamura, and H. Suderow. We thank U. V. Vaidya for his help with magnetization measurements.

¹K. A. McEwen, in *Handbook on Physics and Chemistry of Rare Earths*, edited by K. A. Gschneidner, Jr. and L. Eyring (North-Holland, Amsterdam, 1978), p. 444.

²J. A. White and J. H. Van Vleck, *Phys. Rev. Lett.* **6**, 412 (1961).

³J. H. Van Vleck, *The Theory of Electric and Magnetic Susceptibilities* (Oxford University Press, New York, 1966), p. 246, Sec. 59.

⁴S. K. Malik and R. Vijayaraghavan, *Phys. Lett.* **34A**, 67 (1971).

⁵H. W. de Wijn, A. M. van Diepen, and K. H. J. Buschow, *Phys. Rev. B* **7**, 524 (1973).

⁶K. H. J. Buschow and A. M. van Diepen, *Phys. Rev. B* **8**, 5134 (1973).

⁷S. K. Malik and R. Vijayaraghavan, *Pramana, J. Phys.* **3**, 122 (1974).

⁸H. Adachi, H. Ino, and H. Miwa, *Phys. Rev. B* **59**, 11445 (1999).

⁹A. M. Stewart, *Phys. Status Solidi B* **52**, K1 (1972).

¹⁰H. Adachi, H. Ino, and H. Miwa, *Phys. Rev. B* **56**, 349 (1997).

¹¹H. Adachi and H. Ino, *Nature (London)* **401**, 148 (1999).

¹²P. D. Kulkarni, A. Thamizhavel, V. C. Rakhecha, A. K. Nigam, P. L. Paulose, S. Ramakrishnan, and A. K. Grover, *EPL* **86**, 47003 (2009).

¹³H. J. Williams, J. H. Wernick, E. A. Nesbitt, and R. C. Sherwood, *J. Phys. Soc. Jpn.* **17-B1**, 91 (1962).

¹⁴K. N. R. Taylor, *Adv. Phys.* **20**, 551 (1971).

¹⁵A. K. Grover, S. K. Malik, R. Vijayaraghavan, and K. Shimizu, *J. Appl. Phys.* **50**, 7501 (1979).

¹⁶W. M. Swift and W. E. Wallace, *J. Phys. Chem. Solids* **29**, 2053 (1968).

¹⁷J. Nogués and I. K. Schuller, *J. Magn. Magn. Mater.* **192**, 203 (1999).

¹⁸K. V. Shah, P. Bonville, P. Manfrinetti, A. Provino, and S. K. Dhar, *J. Magn. Magn. Mater.* **321**, 3164 (2009).

¹⁹S. Singh, S. K. Dhar, P. Manfrinetti, A. Palenzona, and D. Mazzone, *J. Magn. Magn. Mater.* **269**, 113 (2004).

²⁰S. K. Dhar, R. Kulkarni, H. Hidaka, Y. Toda, H. Kotegawa, T. C. Kobayashi, P. Manfrinetti, and A. Provino, *J. Phys.: Condens. Matter* **21**, 156001 (2009).

²¹T. I. Ivanova, M. V. Gavrillo, S. A. Nikitin, I. A. Ovchenkova, A. V. Morozkin, D. Badurski, and K. P. Skokov, *J. Magn. Magn. Mater.* **300**, e489 (2006).

²²D. J. Webb, A. F. Marshall, S. Sun, T. H. Geballe, and R. M. White, *IEEE Trans. Magn.* **24**, 588 (1988).

²³P. D. Kulkarni, S. Venkatesh, A. Thamizhavel, V. C. Rakhecha, S. Ramakrishnan, and A. K. Grover, *IEEE Trans. Magn.* **45**, 2902 (2009).

²⁴H. Kanai, N. Noma, and J. Hong, *Fujitsu Sci. Tech. J.* **37**, 174 (2001).